The Permian-Triassic Boundary in the Carnic Alps of Austria (Gartnerkofel Region)			Editors: W.T. Holser & H.P. Schönlaub	
Abh. Geol. B.-A.	ISSN 0378-0864 ISBN 3-900312-74-5	Band **45**	S. 175–192	Wien, Mai 1991

The Permian-Triassic of the Gartnerkofel-1 Core (Carnic Alps, Austria): Statistical Analysis of the Geochemical Data

By KARL STATTEGGER*)

With 15 Text-Figures and 3 Tables

Carinthia
Carnic Alps
Permian/Triassic Boundary
Geochemistry
Multivariate Statistics
Exploratory Data Analysis
Time-Series Analysis

Österreichische Karte 1 : 50.000
Blatt 198

Contents

Zusammenfassung

In der vorliegenden Arbeit wurde das gesamte geochemische Datenmaterial statistisch untersucht, und zwar einmal die ICP-Werte von 18 Variablen von 332 Proben (P. KLEIN, in diesem Band) unter Einschluß der $\delta^{13}C$- und $\delta^{18}O$-Isotopen (M. MAGARITZ & W.T. HOLSER, in diesem Band), zum anderen die INAA-Daten von 25 Variablen von 72 Proben (M. ATTREP et al., in diesem Band).

Zuerst wurden, mit Hilfe der schrittweisen linearen Diskriminanz-Analyse sechs vorgegebene stratigraphisch definierte Probengruppen nach den geochemischen Variablen ausgeschieden. Im ersten Datensatz beruht die Gruppentrennung auf 12 Variablen, nämlich $\delta^{13}C$, P, $\delta^{18}O$, V, Mn, Ba, Ni, S, Zn, Fe, C_{tot} und K. Über 90 % von 332 Proben sind korrekt klassifiziert. Das Diskriminanz-Modell der ersten beiden kanonischen Variablen zeigt klare stratigraphsiche Trends (Abb. 2): Vom basalen Teil des Kerns in der mittleren Bellerophon- Formation bis zum Mazzin-Member nimmt die erste kanonische Variable ab, d.h., es nehmen generell die Werte für $\delta^{13}C$, V, Mn und S ab, wogegen C_{tot} und K ansteigen. Nach einem „Wendepunkt" im Mazzin Member, der den Hauptanomalien entspricht, tritt ein größerer Wechsel im Chemismus ein. Von hier bis zum Beginn des Kerns nimmt die zweite kanonische Variable zu, d. h. es kommt zu einer generellen Zunahme von P, Zn, Fe und zu einer Abnahme von $\delta^{18}O$, Ba und Ni.

Ähnliche Ergebnisse spiegeln die INAA-Daten wider. Aufgrund der geringeren Probenanzahl konnten allerdings nur vier Gruppen unterschieden werden. Dabei tragen die Variablen Eu, Na, U, La, Cr und V signifikant zur Gruppentrennung bei.

Die bedeutendsten geochemischen Variablen wurden in Form von „boxplots" und „3D-plots" stratigraphisch geordnet graphisch dargestellt. Dabei werden sowohl die generelle als auch die wechselseitige stratigraphische Korrelation gezeigt. Diese Methode beweist die starke Zusammengehörigkeit einzelner Variablen aus dem ICP-Datenmaterial in Abhängigkeit von der Li-

*) Author's address: Prof. Dr. KARL STATTEGGER, Geologisch-Paläontologisches Institut, Universität Kiel, Olshausenstraße 40, D-2300 Kiel.

Methode beweist die starke Zusammengehörigkeit einzelner Variablen aus dem ICP-Datenmaterial in Abhängigkeit von der Lithologie. Das gleiche Muster trifft auch für die meisten Variablen im INAA-Datenmaterial zu, die selbst wieder auf einzelne nichtkarbonatische Variablen beziehbar sind.

Die gesamte Datensequenz der relevanten Variablen wurde mit Methoden der Zeitreihenanlayse im Intervall von der obersten Bellerophon Formation bis zum Top des Mazzin Member analysiert. Dabei zeigte sich in den Datenfolgen der einzelnen Variablen ein unruhiger Kurvenverlauf, der von vielen kleinen Oszillationen geprägt ist. Durch Glättung mit ungewichteten gleitenden Mittelwerten kommen aber zwei Anomalien deutlich zum Vorschein: Die erste liegt im basalen Teil des Mazzin Member, die zweite nahe seiner Obergrenze. Nach Autokorrelationsanalysen sind für den Nachweis beider Anomalien $\delta^{13}C$, Mn, Ni und P die entscheidenden Variablen (Abb. 13). Die signifikanten Korrelationen zwischen der unteren und der oberen Anomalie gelten als Hinweis dafür, daß beide Anomalien durch dieselben geochemischen Prozesse zustande kamen. Dabei ist auf jeden Fall eine tektonische Wiederholung von Teilen der angetroffenen Schichtfolge auszuschließen. Auffallend ist eine leichte Verschiebung der Maxima zwischen den Datenfolgen von $\delta^{13}C$ und $\delta^{18}O$, die in der Kreuzkorrelationsanalyse zum Ausdruck kommt und durch das spätere Auftreten der $\delta^{18}O$-Anomalie hervorgerufen wird.

Abstract

The statistical analysis of the geochemical data was performed on two data sets, one containing $\delta^{13}C$ and $\delta^{18}O$ isotopes as well as ICP-data of 18 variables from 332 samples, the other containing INAA-data of 25 variables from 72 samples.

The method of stepwise linear discriminant analysis was used to distinguish among six stratigraphically predefined sample groups. 12 variables contribute significantly to the group-separation in the first data set: $\delta^{13}C$, P, $\delta^{18}O$, V, Mn, Ba, Ni, S, Zn, Fe, C_{tot} and K. More than 90 % of all 332 samples are classified correctly. The discriminant model on the first two canonical variables shows clear stratigraphic trends (Text-Fig. 2): From the basal part of the core (Middle Bellerophon Formation) to the Mazzin Member, the first canonical variable decreases, that means a general decrease of $\delta^{13}C$, V, Mn, S and a general increase of C_{tot}, K. After a "turning point" in the Mazzin Member, corresponding to the main anomalies, we find a major change in the geochemical evolution. From here to the top of the core, the second canonical variable increases, that means a general increase of P, Zn, Fe and a general decrease of $\delta^{18}O$, Ba, Ni. Similar results were obtained from the INAA data-set; only four groups could be distinguished due to the small number of samples. Highest discriminatory power is found in the variables Eu, Na, U, La, Cr and V.

The most important geochemical variables are displayed by box- plots and 3D-plots according to the stratigraphic sample groups. General and individual stratigraphic correlation-patterns are also shown. These patterns indicate strong clustering of some variables of the ICP-data, reflecting the lithology, and of most variables of the INAA-data, which are in turn closely related to some non-carbonatic variables of the ICP-data.

The data-sequences of the relevant variables were analyzed by time-series methods in the interval from the uppermost Bellerophon Formation to the top of the Mazzin Member. The raw data show in part a rugged course caused by many small-scale oscillations. Smoothing by unweighted moving averages makes the two main anomalies easier to recognize. The first anomaly is located at the basal part of the Mazzin Member, the second anomaly near the top of the Mazzin Member. From autocorrelation-analysis, these two main anomalies are most obvious for $\delta^{13}C$, Mn, Ni and P in the correlograms of Text-Fig. 14. The most striking feature is a second positive peak, corresponding to a correlation of the lower anomaly with the upper anomaly caused by similar geochemical processes which were responsible of both anomalies. Nevertheless, there are sufficient differences to reject the hypothesis that the lower and the upper anomalies represent a tectonic repetition of the stratigraphic section. A shift is noticeable between $\delta^{13}C$ and $\delta^{18}O$, proved by crosscorrelation-analysis, due to the later occurrence of the first anomaly in $\delta^{18}O$.

1. Introduction

Chemical study of the Gartnerkofel-core (see Text-Fig. 1) resulted in more than ten thousand elemental and isotopic analyses, carried out at four laboratories as described in other chapters in this volume (M. ATTREP et al., this volume; P. KLEIN, this volume; M. KRALIK, this volume; M. MAGARITZ & W.T. HOLSER, 1989). Some of the interpretations of the various analyses are discussed in the chapters cited, nevertheless it was considered important to make a formal statistical treatment of the entire set of data. The analysis that follows may help to quantify relations that were qualitatively evident in the data sets, and may suggest others that might otherwise go unnoticed. In addition, this rather complete statistical study may serve the reader as a format in which to test newly suggested theoretical relations. Two data-sets were available for the statistical analysis:

1) General geochemical data including C- and O-isotopes of all 332 analyzed core samples, with the 20 variables: $\delta^{13}C$, $\delta^{18}O$, C_{tot}, S, insoluble residue (Res), Al, Ba, Ca, Cr, Fe, K, Mg, Mn, Na, Ni, P, Sr, Ti, V and Zn. Analyses of the elements Al to Zn were of the fraction soluble in 1M HCl (see P. KLEIN, this volume) – mainly the carbonate-fraction, although the levels of elements such as Al and K indicates that some clay minerals were leached. The corresponding data are tabulated by P. KLEIN (this volume).
2) INAA whole-rock analyses of 79 samples with 47 variables. The main problem of this data-set was the many missing values below the detection limit. This was dealt with by the following restrictions: Variables containing more than 10 %, and samples containing more than 4 missing values, were excluded from the statistical treatment (compare B. HITCHON & R.H. FILBY, 1984). The remaining missing values were substituted by one-tenth of the detection limit. Of this data-set, 72 samples were left containing 25 variables: Na, Mg, Al, K, Ca, Sc, Ti, V, Cr, Mn, Fe, Co, Rb, Cs, La, Ce, Sm, Eu, Tb, Dy, Yb, Lu, Hf, Th, U. The corresponding data, but also including some values for As, Sb, Ba, Ta and Ir are tabulated in M. ATTREP et al. (this volume).

The statistical treatment of the geochemical data includes:

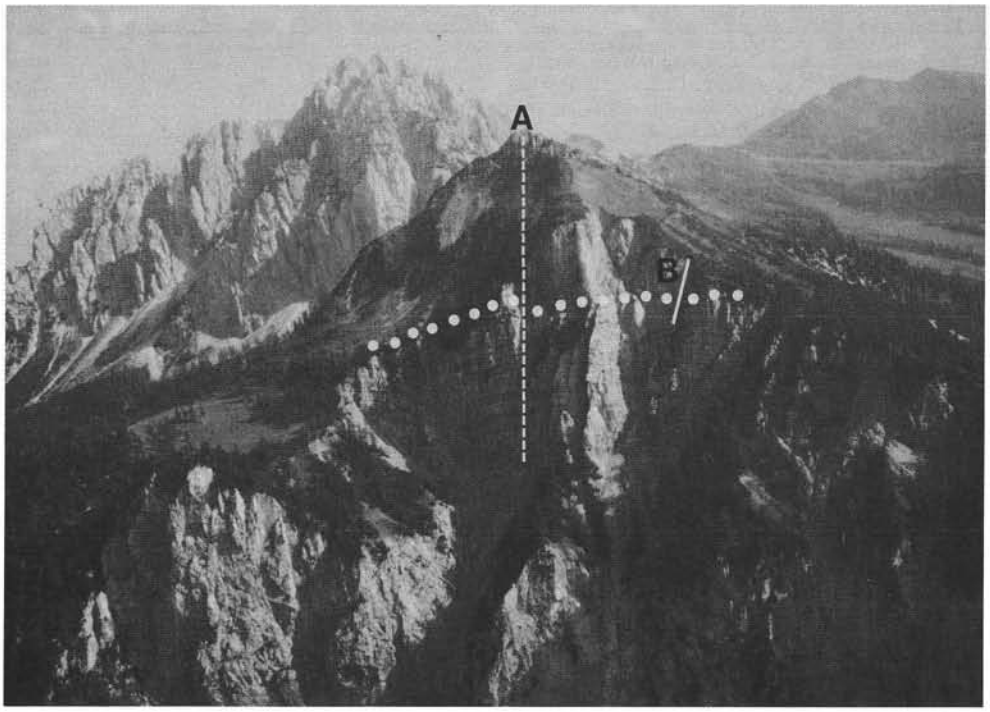

Text-Fig. 1.
Aerial photograph from the north of the Reppwand with the Gartnerkofel (2195 m) in the background.
A: Drill site on Kammleiten (1998 m);
B: Top of the outcrop section.
Dotted line indicates the Permian–Triassic boundary between the Bellerophon Formation (below) and the Werfen Formation above.
Photo: G. FLAJS, Aachen.

- Discrimination among the stratigraphic units using discriminant analysis .
- Characterization of the resulting individual sample-groups by exploratory data-analysis and correlation analysis .
- Analysis of anomalies and events near the Permian/ Triassic boundary for the most sensitive variables by time-series analysis.

2. Geochemical Discrimination Among the Individual Stratigraphic Units

A valuable tool in discrimination among predefined sample groups by their variables is the method of stepwise linear discriminant analysis (R.I. JENNRICH, 1977). It maximizes the differences among the groups by linear classification functions selecting the most discriminating variable among the groups at each step; similarly, a variable will be deleted if its discriminatory power becomes too low. In addition, canonical variables are computed that are composed of coefficients of the original variables and a constant. These canonical variables are the coordinate axes of a multidimensional sample space and allow optimal separation among the sample groups (R.A. REYMENT et al., 1984). The efficiency of the method depends heavily on the data structure of the predefined sample groups (KRZANOWSKI, 1977) because it requires normally distributed variables.

The analysis was performed on both data sets, with six stratigraphically predefined sample groups: Campil Member (unit 4), Seis Member (unit 3B), Mazzin Member (unit 3A), Tesero Horizon (unit 2), Upper Bellerophon Formation (unit 1B), Middle Bellerophon Formation (unit 1A); see Text-Fig. 5 of K. BOECKELMANN (this volume). The boundary between Units 3A and 3B is actually made arbitrarily at the top of the uppermost carbon isotope minimum; a stratigraphic boundary between the Mazzin and Seis members cannot be recognized in the GK-1 core (BOECKELMANN, this volume). Designations of Unit 3A as "Mazzin" and 3B as "Seis" in this chapter are only nominal and for convenience.

2.1. General Geochemistry

First, the 20 variables were checked for normality by normal probability plots and the Kolmogorov-Smirnow

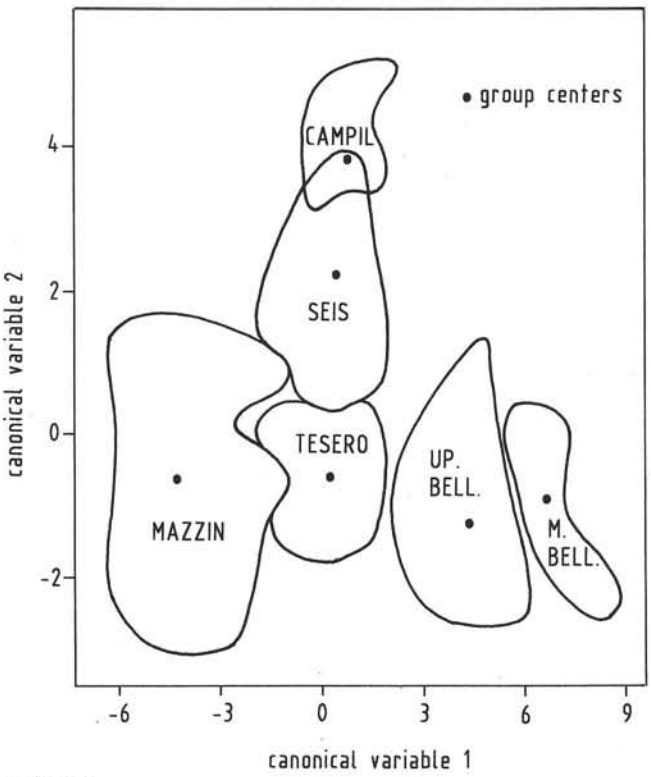

Text-Fig. 2.
Discriminant model of the general geochemistry data-set showing optimal separation among six stratigraphic units (cf. Table 1) in relation to the first and second canonical variable .

Table 1.
Main results from the discriminant analysis of the general geochemistry data-set.

Discriminant variables with F-values:

$\delta^{13}C$	P	$\delta^{18}O$	V	Mn	Ba	Ni	S	Zn	Fe	C_{tot}	K
484.64	48.44	38.47	32.46	17.08	16.66	13.44	12.32	10.59	7.93	7.59	7.21

$F_{99,9\%}$ = 4.25 degrees of freedom = 5,314

F-matrix of group separation

degrees of freedom = 13,314

$F_{99,9\%}$ = 2.80

	CAMPIL	SEIS	MAZZIN	TESERO	U.BELL
SEIS	7.90				
MAZZIN	51.31	106.94			
TESERO	25.15	22.33	52.05		
U.BELL	39.84	69.83	226.27	41.18	
M.BELL	53.25	81.62	232.47	58.94	15.52

U.BELL=Upper Bellerophon; M.BELL=Middle Bellerophon

classification-matrix

number of cases classified into group

	CAMPIL	SEIS	MAZZIN	TESERO	U.BELL	M.BELL
CAMPIL	15	2	0	0	0	0
SEIS	9	64	0	2	0	0
MAZZIN	0	0	120	1	0	0
TESERO	0	0	0	29	0	0
U.BELL	0	0	0	2	54	2
M.BELL	0	0	0	0	1	31

% of correctly classified samples

CAMPIL	SEIS	MAZZIN	TESERO	U.BELL	M.BELL
88	85	99	100	97	94

canonical variables

$$V_1 = 2.868\delta^{13}C + 0.278P - 0.078\delta^{18}O + 1.686V + 0.003Mn + 0.027Ba - 0.215Ni + 1.128S + 0.248Zn - 0.652Fe - 0.788C - 1.274K - 4.197$$

$$V_2 = 0.857\delta^{13}C + 3.759P - 0.380\delta^{18}O - 0.568V + 0.001Mn - 0.653Ba - 0.854Ni - 0.404S + 1.290Zn + 2.426Fe - 0.380C + 0.638K - 13.274$$

test: C_{tot}, S, insoluble residue, Al, Ba, K, Ni, P, V and Zn follow a lognormal distribution, the other variables are normally distributed. Therefore, logarithms of the lognormally distributed variables were used instead of the raw data. Six sample groups were predefined according to the stratigraphic units in the core.

Main results are summarized in Table 1 and Text-Fig. 2. 12 variables contribute essentially to the very distinct group separation, ordered with decreasing significance: $\delta^{13}C$, P, $\delta^{18}O$, V, Mn, Ba, Ni, S, Zn, Fe, C_{tot}, K. Group separation is statistically significant at a very high level. The only overlap, with the lowest F-value of group separation, can be observed between Seis and Campil: some samples from the upper part of the Seis-member are classified as Campil, indicating a transition stage between these two units, as was recognized in defining these units (K. BOECKELMANN, this volume). This overlap can also seen from the classification matrix which indicates the classification pattern of all samples into the six groups. In general, more than 90 % of all samples are classified correctly, up to 100 % in the Tesero Horizon. The coefficients of the two most powerful canonical variables are also listed.

The canonical variables are used as coordinate axes in the two-dimensional discriminant model of Text-Fig. 2. The graph shows the areas covered by more than 95 % of the samples within the individual groups and the group centers. Increasing values on the first canonical variable correspond mainly to increasing contents of $\delta^{13}C$, V, Mn, S and decreasing contents of C_{tot} and K, increasing values on the second canonical variable to increasing contents of P, Zn, Fe and decreasing contents of $\delta^{18}O$, Ba, Ni. The group-distribution pattern shows clear time-trends: From Middle Bellerophon to Mazzin, the first canonical variable goes down, from Mazzin to Campil, the second canonical variables goes up.

2.2. INAA Data

The INAA data were processed in the same way as the first data set. Tests of normality showed that Fe, Co and Cs were log- normally distributed variables. Only four stratigraphical groups could be predefined due to the small number of samples: Bellerophon Formation (units 1A, B), Tesero Horizon (unit 2), Mazzin Member (unit 3A), Seis/Campil Members (units 3B, 4).

Results of discriminant analysis are given in Table 2 and Text-Fig. 3. Group separation is based mainly on six variables (in decreasing order of significance): Eu, Na, U, La, Cr, V. Separation among the four groups is highly significant. Only one sample of all 72 failed correct classification in the classification matrix. This sample of the Tesero Horizon is classified as Mazzin.

The plot of the samples on the first and the second canonical variable in Text-Fig. 3 shows the very clear group separation. The first canonical variable corresponds mainly to U and Cr, the second to Eu. The group distribution pattern is similar to the pattern of general geochemistry with similar time trends. A decrease in the first canonical variable from Bellerophon to Mazzin is followed by an increase in the second ca-

Table 2.
Main results from the discriminant analysis of the INAA data-set.

Discriminant variables with F-values:

Eu	Na	U	La	Cr	V
16.32	15.43	15.34	13.76	8.75	6.77

$F_{99,9\%}$ = 6.19 degrees of freedom = 3,59

F-matrix of group separation

degrees of freedom = 25,44

	CAMPIL/SEIS	MAZZIN	TESERO
MAZZIN	5.80		
TESERO	3.30	3.66	
BELLEROPHON	9.52	16.43	6.89

$F_{99,9\%}$ = 2.95

classification-matrix

	number of cases classified into group CAMPIL/SEIS	MAZZIN	TESERO	BELLEROPHON
CAMPIL/SEIS	19	0	0	0
MAZZIN	0	38	0	0
TESERO	0	1	6	0
BELLEROPHON	0	0	0	8

% of correctly classified samples	CAMPIL/SEIS	MAZZIN	TESERO	BELLEROPHON
	100	100	86	100

canonical variables

$V_1 = 0.181Eu - 0.004Na + 0.560U - 0.352La + 0.105Cr - 0.080V - 0.053$

$V_2 = 10.313Eu - 0.002Na + 0.056U - 0.173La + 0.018Cr - 0.007V - 4.557$

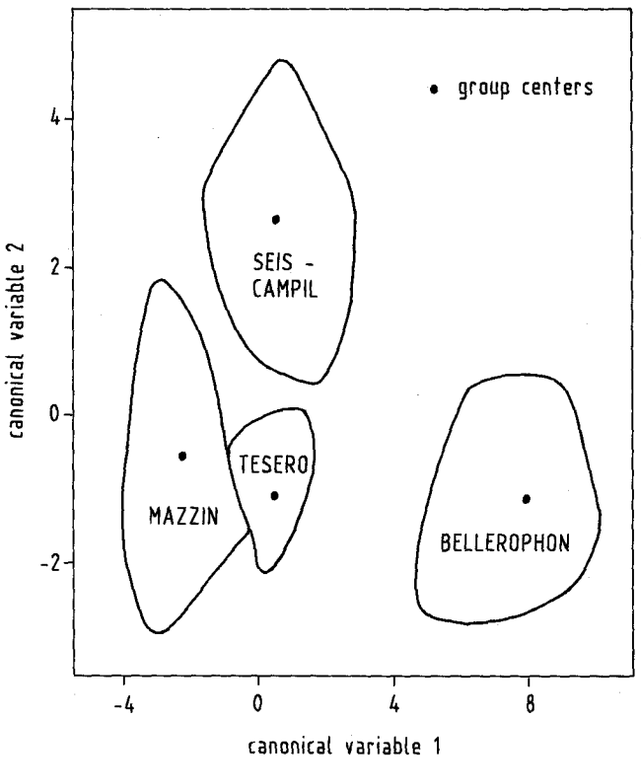

Text-Fig. 3.
Discriminant model of the INAA data-set showing optimal separation among six stratigraphic units (cf. Table 2) in relation to the first and second canonical variable).

nonical variable from Mazzin to Seis/Campil. The Bellerophon samples are most separated from the other groups, Tesero and Mazzin are closest together.

2.3. Summary Remarks

The use of linear discriminant analysis shows a clear separation of the individual stratigraphic units for both data sets. The most sensitive variables of geochemical changes and instabilities near the Permian/Triassic boundary are $\delta^{13}C$, P, $\delta^{18}O$, V, Mn, Eu, Na, U, whereas the "lithological" variables like Ca, Mg or insoluble residue do not contribute to the stratigraphic group separation. Geochemical time trends, expressed by the canonical variables, exhibit a similar evolution pattern in both data sets (compare Text-Figs. 2 and 3). We find a "turning point" in the Mazzin member, probably corresponding to the two main anomalies. Here, a major change in the geochemical evolution occured. The decrease of a specific linear combination of the geochemical variables turned to an increase in another linear combination of these variables.

3. Characterization of the Stratigraphic Units

Following the general discrimination-pattern of the stratigraphic units modeled by discriminant analysis, the individual units are analyzed using
- exploratory data analysis
- correlation analysis.

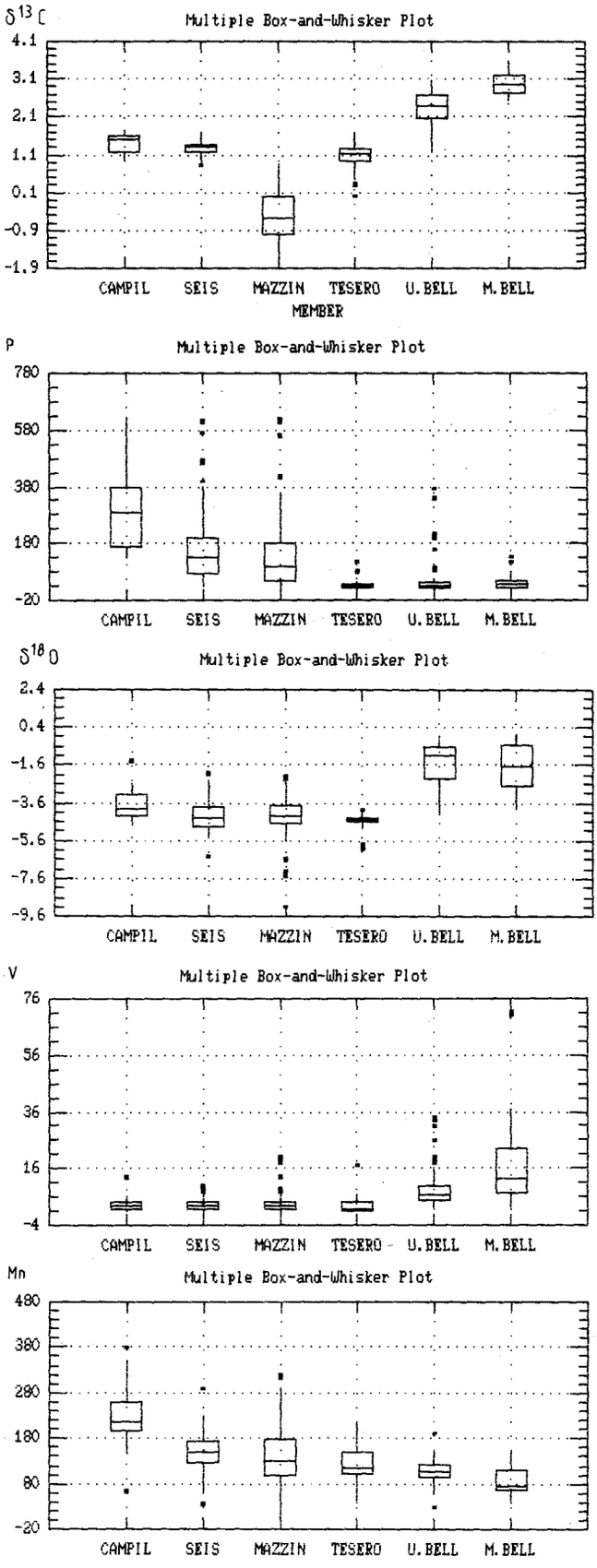

Text-Fig. 4.
Multiple box-plots of the variables with the highest discriminatory power among the stratigraphic units (general geochemistry): $\delta^{13}C$, P, $\delta^{18}O$, V, Mn. The box delimits the second and third quartiles around the median, the "whisker" extensions delimit the total range of the first and fourth quartiles, or, if outliers are present which are marked by dots, 1.5 times the range of the box on each side.

3.1. Exploratory Data Analysis

Exploratory data analysis describes the variables of a data set in an ordinary general manner. No theoretical data distribution is required. Therefore, one can compare easily several variables in a data set or one variable in several data sets (compare P.F. VELLEMAN & D.C. HOAGLIN, 1981).

Of most interest are the variables of high discriminatory power (compare Tables 1 and 2). These variables are displayed in the multiple box plots of Text-Fig. 4 (general geochemistry) and Text-Fig. 5 (INAA data).

The box plot is an effective way to display univariate summary statistics graphically. The plot divides the data into four areas, the quartiles. The second and the third quartile are in the box separated by the median-line, the first and the fourth quartile are the linear extensions ("whiskers") of the box. Additional outliers beyond or above the extensions are marked by dots. With these features, the box-plot allows one to describe very easily the data structure, to detect outliers and to note asymmetric behaviour of a variable.

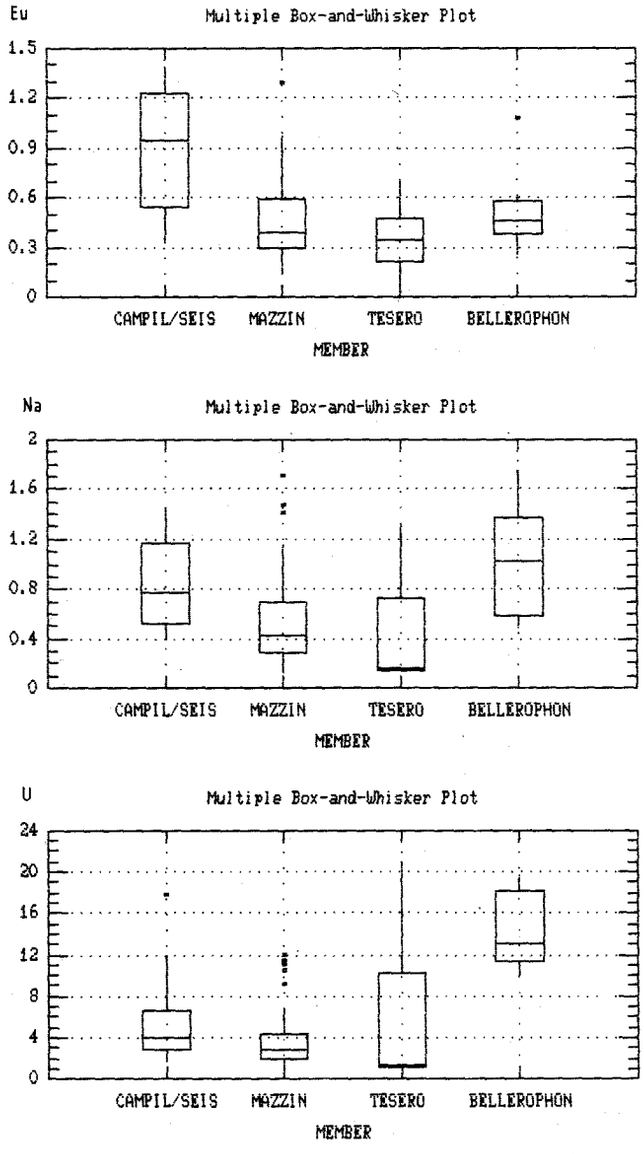

Text-Fig. 5.
Multiple box-plots of the INAA variables with the highest discriminatory power among the stratigraphic units: Eu, Na, U.

In Text-Fig. 4, $\delta^{13}C$ shows the greatest differences among the six groups: it was used in defining the "stratigraphic units". P follows a clear trend with increasing values going up the stratigraphic sequence, $\delta^{18}O$ is high in the Permian and low in the Triassic (including Tesero) samples, V has also higher values in the Permian samples. Mn follows a stratigraphic-upward- increasing trend like P. Differences among the stratigraphic units are not so clear for the other variables in the general geochemistry set.

For the INAA data (Text-Fig. 5), noticeable differences among the four stratigraphic units can be observed in the multiple box-plots of Eu, Na and U by generally lowered contents in the Tesero horizon and the Mazzin member.

The box-plots of $\delta^{13}C$, P and $\delta^{18}O$ are summarized in 3D- plots using the three variables as coordinate axes. Text-Fig. 6 contains plots of all 332 samples, and of each individual stratigraphic unit. In a similar way, the plots of Text-Fig. 7 summarize the box-plots of Eu, Na and U.

3.2. Correlation Analysis

3.2.1. General Geochemistry

The general correlation-pattern of all 332 samples, using the raw data of $\delta^{13}C$, $\delta^{18}O$, Ca, Cr, Fe, Mg, Mn, Na, Sr, Ti and log-transformed data of C_{tot}, S, insoluble residue (Res), Al, Ba, K, Ni, P, V, Zn, is shown in Text-Fig. 8. The plot contains only those correlations above the 99 % significance level of the product-moment correlation coefficient which are also significant within the individual groups. Significance is tested against the normal distribution of correlation coefficients (see E. KREYSZIG, 1979). This test is more restrictive than the commonly used significance tables and requires higher correlations for significance.

The general correlation pattern comprises the following pairs of variables:

Positive correlations: C_{tot} – Ca, C_{tot} – Mg, Res – Al, Res – Ba, Res – K, Res – P, Al – Ba, Al – K, Al – P, Al – Ti, Ba – K, Ba – P, Ca – Mg, K – P.

Negative correlations: C_{tot} – Res, C_{tot} – Al, C_{tot} – K, C_{tot} – P, Res – Ca, Res – Mg, Al – Ca, Al – Mg, Ba – Ca, Ba – Mg, Ca – K, Ca – P, K – Mg, Mg – P.

Thereof, two clusters of variables result:

❶ Res – Al – Ba – K – P.
❷ C_{tot} – Ca – Mg.

These two clusters can be easily referred to the general lithology of the Gartnerkofel core: clastic and carbonatic sediments.

The correlations of the main lithological variables, Res – Ca – Mg – C_{tot}, are probably spurious, because these four variables contain the highest percentages of the data set and may be affected by the constant sum constraint (J. AITCHISON, 1988). Nevertheless, these variables do not contribute much to the group separation in the discriminant analysis. The other variables are supposed to be independent, except the correlations to the four variables mentioned above, they do not form a closed data array. For the six individual

Table 3.
Correlation matrices of the individual stratigraphic units.
Positively significant correlations not contained in the general correlation pattern of Text-Fig. 8 are framed.

CAMPIL

	$\delta^{18}O$	$\delta^{13}C$	C	S	Res	Al	Ba	Ca	Cr	Fe	K	Mg	Mn	Na	Ni	P	Sr	Ti	V	Zn
$\delta^{18}O$	1.00000																			
$\delta^{13}C$	-.62457	1.00000																		
C	-.33323	-.12484	1.00000																	
S	-.11246	-.20819	.69308	1.00000																
Res	.21315	.24507	-.90707	-.59957	1.00000															
Al	-.27286	.27153	-.35439	-.31945	.49040	1.00000														
Ba	-.00310	.39136	-.78363	-.62125	.88411	.68942	1.00000													
Ca	-.33699	-.14468	.96002	.69053	-.94787	-.37288	-.85379	1.00000												
Cr	-.28254	-.00915	.10157	-.13554	-.02824	.75473	.22142	.08958	1.00000											
Fe	-.02107	-.11957	.68374	.24332	-.62666	-.11076	-.43474	.64214	.30078	1.00000										
K	-.12561	.18440	-.56481	-.52619	.64355	.92710	.78734	-.57847	.67590	-.21718	1.00000									
Mg	-.40540	-.09515	.94483	.59527	-.91512	-.30853	-.81237	.97463	.14856	.68105	-.51037	1.00000								
Mn	.20257	-.28699	.63348	.37167	-.51346	-.25437	-.36495	.49545	.10832	.78570	-.32856	.45400	1.00000							
Na	-.43969	.32510	.27255	-.02590	-.39572	.17990	-.06647	.31317	.38051	.33864	.14624	.31002	.03638	1.00000						
Ni	-.10110	-.07990	.16483	-.14507	-.02180	.34826	-.01843	.04550	.41905	.19342	.25902	.20508	.08176	-.05825	1.00000					
P	.42839	.04624	-.73191	-.59255	.75615	.33343	.76688	-.85081	.08900	-.31160	.54007	-.83491	-.08675	-.13226	.06273	1.00000				
Sr	-.05991	-.32536	.86447	.52647	-.94727	-.58999	-.84708	.84763	-.06193	.63798	-.72046	.82096	.62253	.29058	.07064	-.60071	1.00000			
Ti	-.21287	.01547	-.05379	-.16476	.14969	.87401	.38557	-.09304	.91825	.17383	.78538	-.03389	.04178	.31677	.50000	.21739	-.22402	1.00000		
V	-.42604	.24075	.34650	.19031	-.16267	.49543	.20023	.20964	.63477	.41397	.41081	.22127	.44759	.54736	.22324	.12884	.11556	.63104	1.00000	
Zn	-.29354	-.31884	.61739	.75896	-.54162	-.10705	-.53339	.60546	.04911	-.00246	-.31122	.56477	.11446	-.01921	.17160	-.64014	.47431	.03570	.15903	1.00000

SEIS

	$\delta^{18}O$	$\delta^{13}C$	C	S	Res	Al	Ba	Ca	Cr	Fe	K	Mg	Mn	Na	Ni	P	Sr	Ti	V	Zn
$\delta^{18}O$	1.00000																			
$\delta^{13}C$	.50154	1.00000																		
C	.02890	-.18460	1.00000																	
S	.17066	-.04399	-.29282	1.00000																
Res	.09451	.17854	-.74742	.63247	1.00000															
Al	.04194	.22495	-.61422	.55371	.76121	1.00000														
Ba	.00927	.14493	-.60636	.58671	.83924	.75447	1.00000													
Ca	.02892	-.23172	.84361	-.32265	-.81428	-.77471	-.73155	1.00000												
Cr	.18085	.19606	-.13486	.66597	.40598	.47205	.49449	-.27133	1.00000											
Fe	.02585	-.00252	.04795	.15052	.10712	.08294	.06324	.08049	.17826	1.00000										
K	.06141	.21049	-.64744	.58386	.84058	.90253	.82673	-.75880	.48033	.06416	1.00000									
Mg	.10146	-.02983	.84881	-.41373	-.73811	-.65597	-.59375	.76847	-.18832	-.06905	-.67232	1.00000								
Mn	.14552	-.18982	.19226	.25459	.08498	-.03723	.02785	.15476	.19960	.71319	-.05738	.07014	1.00000							
Na	.26855	.24085	.07647	.12282	.01976	.22975	.04377	.05571	.18885	-.03907	.25210	.06251	-.08674	1.00000						
Ni	.15918	-.01433	-.17556	.40260	.37472	.25189	.50851	-.20448	.43718	.01576	.38783	-.14679	.01354	.12186	1.00000					
P	.08020	.17155	-.72104	.55996	.90220	.69387	.77497	-.77740	.42870	.16171	.77500	-.75759	.15079	.06982	.41049	1.00000				
Sr	-.10636	-.29673	.20735	.02735	-.34468	-.35140	-.31486	.50448	-.12609	-.00119	-.31838	-.05516	-.02548	-.00189	-.06851	-.24361	1.00000			
Ti	-.02152	.02330	-.30550	.46640	.37533	.72714	.43886	-.43576	.57998	.11941	.58744	-.37885	.05212	.21508	.09696	.37340	-.15691	1.00000		
V	-.03000	-.17574	.26460	.39398	.15263	.22175	.12662	.05246	.31370	.31814	.17749	-.00763	.42646	.05443	.08364	.21393	.06046	.41526	1.00000	
Zn	.00547	-.15588	.09596	-.10701	-.19790	-.17349	-.17184	.21145	-.12852	.32656	-.16264	.10110	.25034	.00348	-.12924	-.18176	.04927	.06656	.08213	1.00000

MAZZIN

	$\delta^{18}O$	$\delta^{13}C$	C	S	Res	Al	Ba	Ca	Cr	Fe	K	Mg	Mn	Na	Ni	P	Sr	Ti	V	Zn
$\delta^{18}O$	1.00000																			
$\delta^{13}C$	.14774	1.00000																		
C	.21542	.22149	1.00000																	
S	-.13113	-.71768	-.52914	1.00000																
Res	-.29494	-.54096	-.65647	.70995	1.00000															
Al	-.12321	-.15249	-.59289	.27256	.60787	1.00000														
Ba	-.21369	-.26092	-.48340	.35271	.71085	.65643	1.00000													
Ca	.14536	.25274	.83373	-.53505	-.79837	-.63114	-.57278	1.00000												
Cr	-.05459	.05312	-.31126	.14074	.39466	.56958	.39692	-.41349	1.00000											
Fe	-.14476	-.32935	-.63833	.49707	.40399	.42679	.29178	-.42091	.24890	1.00000										
K	-.19235	-.25814	-.61566	.43578	.77189	.93257	.72002	-.68718	.57411	.41863	1.00000									
Mg	.37881	.34712	.81440	-.61406	-.77263	-.55335	-.57317	.69872	-.33722	-.40785	-.66796	1.00000								
Mn	-.24252	-.44319	.13408	.24796	.32950	.20328	.35210	-.03460	.08338	.21530	.25329	-.07844	1.00000							
Na	.16630	-.13189	.01001	-.02000	.10638	.34453	.19445	-.02885	.25252	.01905	.30677	-.05747	.18962	1.00000						
Ni	-.40154	-.19311	-.46341	.34307	.54585	.56161	.47949	-.44752	.39095	.41486	.63349	-.55745	.26211	.15888	1.00000					
P	-.31177	-.56382	-.58616	.64131	.80592	.56926	.61001	-.64677	.18270	.46400	.65640	-.67482	.44679	.11475	.57457	1.00000				
Sr	-.22224	-.05629	.11539	.06642	-.12332	-.21780	-.07633	.44471	-.10966	-.14395	-.13300	-.25286	-.07829	-.02351	-.01035	-.14257	1.00000			
Ti	.05244	.09002	-.25778	-.04508	.22311	.73758	.39164	-.30059	.64038	.16720	.64797	-.25221	.01895	.52294	.29254	.09371	-.09254	1.00000		
V	.05180	-.56141	-.32871	.52454	.64066	.53497	.54552	-.39982	.28413	.39142	.61859	-.35243	.33294	.34092	.29538	.56012	-.08806	.30343	1.00000	
Zn	-.10456	.17992	-.17580	-.16669	.00381	.38122	.23892	-.11052	.27938	.03465	.35090	-.17879	.02949	.20513	.20461	-.02875	.01726	.44007	-.12161	1.00000

Table 3 (continued).

TESERO

	$\delta^{18}O$	$\delta^{13}C$	C	S	Res	Al	Ba	Ca	Cr	Fe	K	Mg	Mn	Na	Ni	P	Sr	Ti	V	Zn
$\delta^{18}O$	1.00000																			
$\delta^{13}C$	-.22484	1.00000																		
C	.65911	-.06645	1.00000																	
S	-.63073	.03065	-.53111	1.00000																
Res	-.58811	.07073	-.65363	.53558	1.00000															
Al	-.63705	.09305	-.88440	.56156	.79875	1.00000														
Ba	-.58464	-.10966	-.65254	.67273	.75325	.71926	1.00000													
Ca	.71211	-.09325	.97197	-.54682	-.71991	-.87445	-.67504	1.00000												
Cr	-.56561	.14494	-.95263	.40732	.65887	.91155	.60169	-.90633	1.00000											
Fe	-.45690	-.26220	-.79186	.29668	.23223	.57789	.34396	-.70166	.72016	1.00000										
K	-.62379	.14860	-.81721	.51534	.87435	.95724	.74672	-.82817	.86656	.43067	1.00000									
Mg	.74473	-.06824	.94770	-.53678	-.75568	-.91355	-.72019	.94942	-.91687	-.70198	-.89632	1.00000								
Mn	.33442	-.76078	.50874	-.30335	-.44026	-.52574	-.20320	.51548	-.56954	-.02681	-.54753	.44883	1.00000							
Na	-.45424	.05635	-.90849	.51733	.41574	.73992	.53197	-.83762	.85553	.77707	.62884	-.75797	-.48942	1.00000						
Ni	-.69455	.35325	-.69248	.50247	.72856	.83144	.60328	-.71673	.75751	.34028	.87414	-.82694	-.56179	.47043	1.00000					
P	-.59342	-.05462	-.69886	.35707	.75450	.82119	.68640	-.72425	.72451	.44206	.89073	-.81263	-.24950	.48908	.72251	1.00000				
Sr	.45478	.18276	.82651	-.33451	-.38387	-.62615	-.37415	.82780	-.72450	-.83858	-.50543	.76146	.18918	-.72236	-.41536	-.45027	1.00000			
Ti	-.47757	.02652	-.95303	.42639	.60362	.86971	.57491	-.88964	.96121	.76527	.79895	-.86310	-.53038	.92182	.61510	.65645	-.76998	1.00000		
V	-.49723	.10098	-.57620	.50017	.83262	.76541	.77490	-.58471	.66724	.20150	.86918	-.68452	-.41023	.39178	.73303	.77722	-.21580	.60047	1.00000	
Zn	-.76314	-.16686	-.54301	.52453	.34255	.52974	.49081	-.52714	.45301	.63349	.43080	-.57848	.09763	.42367	.47491	.50632	-.48623	.40408	.32403	1.00000

UPPER BELLEROPHON

	$\delta^{18}O$	$\delta^{13}C$	C	S	Res	Al	Ba	Ca	Cr	Fe	K	Mg	Mn	Na	Ni	P	Sr	Ti	V	Zn
$\delta^{18}O$	1.00000																			
$\delta^{13}C$	.73833	1.00000																		
C	-.25717	-.18264	1.00000																	
S	.16661	-.04662	-.69693	1.00000																
Res	.11394	-.04271	-.66462	.69602	1.00000															
Al	.33571	.24200	-.66222	.60266	.67916	1.00000														
Ba	.04539	.02386	-.42271	.39611	.54482	.50129	1.00000													
Ca	-.33076	-.21994	.95309	-.62238	-.72088	-.66451	-.44993	1.00000												
Cr	-.22587	-.21132	.04273	.18732	.33599	.34094	.31555	.01100	1.00000											
Fe	.52782	.33469	-.16383	.35428	.41170	.51098	.19075	-.25802	.09030	1.00000										
K	.33394	.17905	-.62377	.66622	.78364	.93758	.53521	-.65131	.36070	.58571	1.00000									
Mg	-.03311	.04118	.91361	-.63278	-.75809	-.62314	-.45591	.91142	-.08726	-.07762	-.59638	1.00000								
Mn	.37318	.40013	.48239	-.31058	-.21992	-.12756	-.16848	.40817	.12355	.48786	-.06969	.58027	1.00000							
Na	.26870	.18027	.09282	.14339	.19006	.47892	.10807	.05740	.37992	.51061	.47176	.13314	.34505	1.00000						
Ni	.45740	.42547	-.59407	.43976	.40298	.71427	.39148	-.54772	.21336	.27965	.62060	-.44746	-.05186	.29313	1.00000					
P	.17299	.15076	-.81537	.58270	.83423	.68759	.60761	-.85038	.14465	.27141	.71743	-.84775	-.39208	.00689	.50414	1.00000				
Sr	-.55476	-.41477	.72483	-.46779	-.46307	-.59536	-.31267	.76995	-.00691	-.42270	-.56231	.56096	.09512	.01759	-.59897	-.59603	1.00000			
Ti	-.25091	-.14809	-.02727	.23097	.25950	.46605	.07505	-.03194	.46868	.25872	.44723	-.08835	.07128	.55631	.13093	.06093	.05456	1.00000		
V	-.38912	-.11302	.33363	-.20056	-.26508	-.23499	.02574	.36736	.31278	-.26317	-.22574	.30549	.01132	-.14888	-.05208	-.22108	.28809	.01822	1.00000	
Zn	.33631	.31866	-.16144	.07706	-.06116	.26794	.09521	-.08380	.00877	.08186	.18788	.03689	.19213	.12816	.36622	-.04086	-.18228	.11748	-.05412	1.00000

MIDDLE BELLEROPHON

	$\delta^{18}O$	$\delta^{13}C$	C	S	Res	Al	Ba	Ca	Cr	Fe	K	Mg	Mn	Na	Ni	P	Sr	Ti	V	Zn
$\delta^{18}O$	1.00000																			
$\delta^{13}C$	.87958	1.00000																		
C	.16040	.12411	1.00000																	
S	.16050	.15292	-.78166	1.00000																
Res	-.15143	-.24863	-.75678	.70585	1.00000															
Al	-.06693	-.12546	-.87015	.82199	.86713	1.00000														
Ba	.18813	.19510	-.59475	.77557	.69952	.71312	1.00000													
Ca	.22310	.17930	.95521	-.80677	-.79258	-.90362	-.64339	1.00000												
Cr	.16096	.05599	-.14204	.37226	.41988	.22415	.44818	-.21615	1.00000											
Fe	-.18993	-.07627	-.88134	.72611	.67200	.69587	.66871	-.85158	.21507	1.00000										
K	-.12697	-.17707	-.82497	.77124	.90712	.94008	.74110	-.85395	.24001	.72807	1.00000									
Mg	.19812	.21073	.86968	-.76997	-.73803	-.89428	-.59927	.90156	-.15342	-.75364	-.87408	1.00000								
Mn	.01656	.13606	-.19804	.19530	.15066	.00027	.35560	-.17475	.33772	.57445	.14199	-.11059	1.00000							
Na	.49590	.62667	.09912	.30056	-.18103	.02787	.33088	.06279	.16387	-.05230	-.03083	.05319	-.02405	1.00000						
Ni	.16555	.15744	-.45787	.60490	.63224	.59440	.63626	-.49047	.37583	.46090	.57773	-.42938	.13912	.26032	1.00000					
P	-.28091	-.40895	-.69900	.70192	.81136	.82309	.55984	-.75803	.34453	.57438	.79696	-.73464	-.00930	-.14424	.54782	1.00000				
Sr	.19811	.36856	.34375	.00400	-.37474	-.22293	.17811	.23288	.14323	-.23112	-.26645	.27713	-.03761	.80389	.05721	-.20755	1.00000			
Ti	-.22314	-.32356	-.47869	.64294	.70731	.65246	.69173	-.58971	.36314	.50489	.65849	-.48347	.20584	.03750	.49201	.73471	.07082	1.00000		
V	-.26484	-.45405	.32337	-.41814	-.12487	-.21517	-.43016	.25583	.09654	-.44174	-.26253	.14372	-.37311	-.45879	-.22941	-.05031	-.20884	-.17498	1.00000	
Zn	.27150	.46336	-.45524	.62965	.42088	.40380	.69255	-.47245	.26192	.66525	.42107	-.35729	.51378	.41385	.61289	.26048	.21889	.34366	-.59300	1.00000

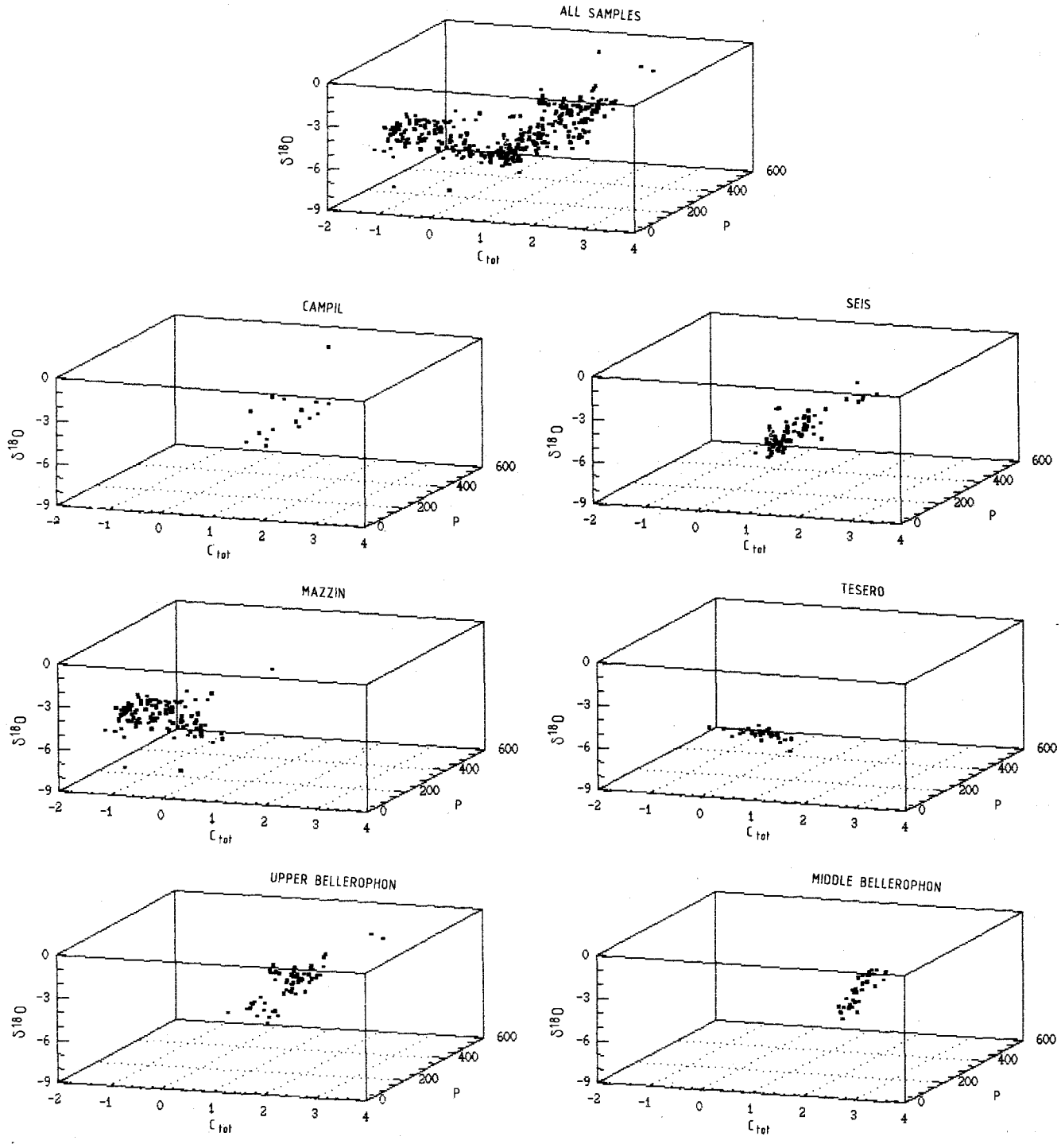

Text-Fig. 6.
3-D-plots on $\delta^{13}C$, P and $\delta^{18}O$ of all 332 samples (general geochemistry) and of the individual stratigraphic units.

stratigraphic units, the correlation matrices are given in Table 3. Specific significant positive correlations which do not belong to the general correlation structure are framed.

The stratigraphic correlation pattern in Text-Fig. 9 contains the specific significant positive correlations in a stratigraphic order. Most changes occur at the Tesero Horizon and the Mazzin member.

3.2.2. INAA Data

The plot of the general correlation structure of the 25 INAA variables in Text-Fig. 10 shows very strong clustering of the major part of the variables with significant positive correlations. This cluster is formed by Na, Al, K, ,Sc, Ti, V, Cr, Rb, Cs, La, Ce, Sm, Eu, Tb, Dy, Yb, Lu, Hf, Th. Weaker affinities to that cluster are shown by Co and U. Ca and Mg form a second cluster. Fe is significantly correlated to Co, Mn has no significant corre lations to the other variables.

No specific significant positive correlations could be observed within the individual sample groups due to that strong general clustering and due to the small number of samples, especially in the Bellerophon Member and the Tesero Horizon.

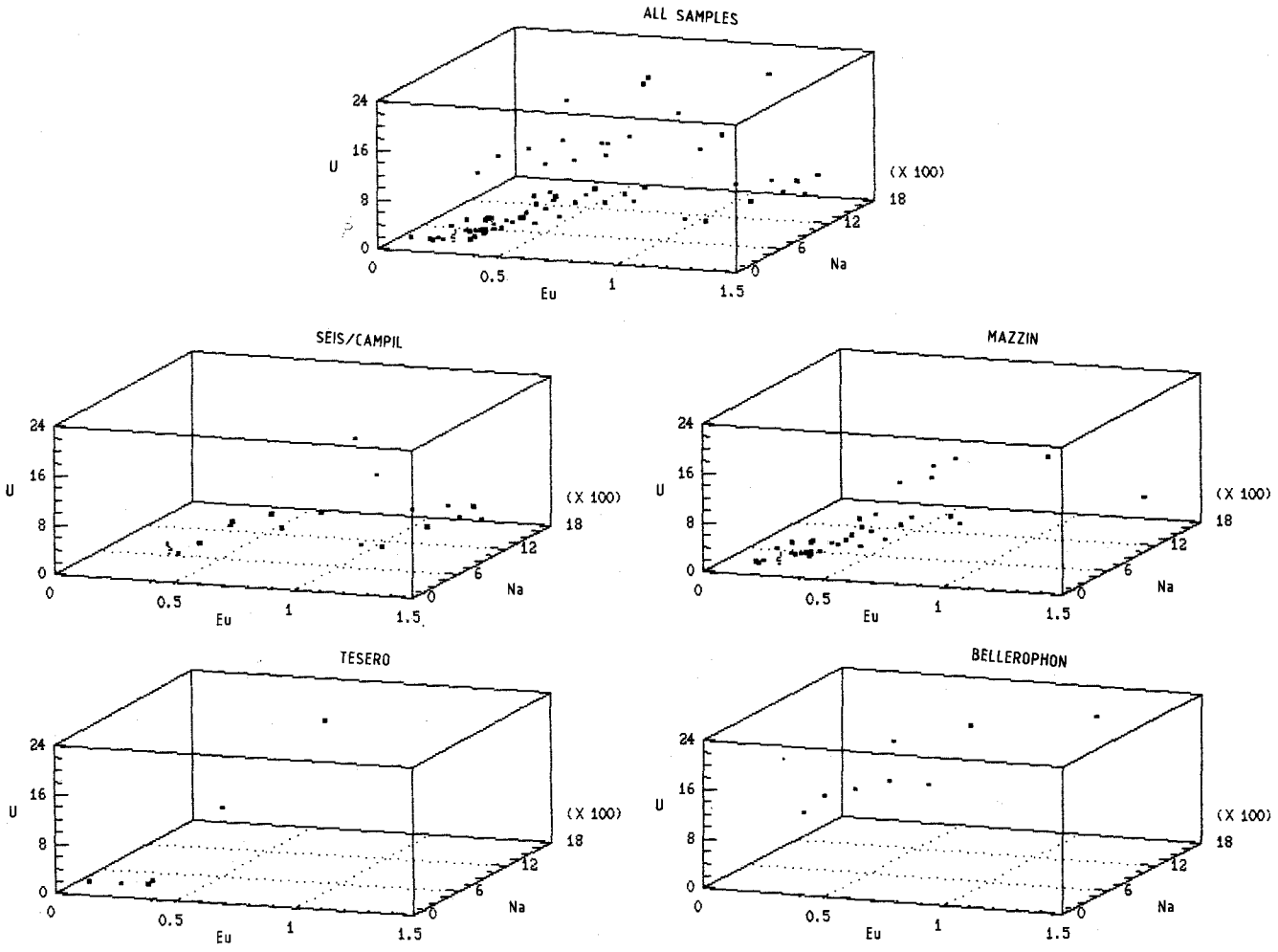

Text-Fig. 7.
3-D-plots on Eu, Na and U of all 72 INAA-samples and of the individual stratigraphic units.

3.2.3. Correlations Between the Two Data Sets

The general correlation pattern of isotopes, ICP and INAA data, restricted to the 72 INAA samples is shown in Text-Fig. 11. The strong clustering effect of the variables within the two data sets is maintained. The ICP cluster Res – Al – Ba – K – P has significant positive correlations to the INAA cluster Na – Al – K – Sc – Ti – V – Cr – Rb – Cs – La – Ce – Sm – Eu – Tb – Dy – Yb – Lu – Hf – Th and significant negative correlations to the INAA cluster Ca – Mg. In contrary, the ICP cluster C_{tot} – Ca – Mg has significant positive correlations to the corresponding INAA cluster Ca – Mg and negative significant correlations to the other INAA cluster. Noticeable is the absence of significant positive correlations, concerning the same element with ICP and INAA, for Na, Ti, V and Cr, whereby Ti and Cr are near the 99 % significance level. Therefore, the INAA data can not be seen as a subset of the ICP data for these variables (compare the partly different discriminatory power in the discriminant analyses of the two data sets, section 2).

4. Time Series Analysis

The aim of analyzing geochemical variables of the Gartnerkofel core by time series methods is to get a closer look at the vertical succession composing a data sequence. Variations in time in relation to the main geochemical anomalies are of special interest. Time series analysis is restricted to the relevant variables of the general geochemical data set, $\delta^{13}C$, $\delta^{18}O$, C_{tot}, S, Ba, Fe, K, Mn, Ni, P, V, Zn in the interval from the uppermost Bellerophon formation to the top of the Mazzin member (samples 215 to 93), containing 160 samples in an interval of 62.74 meters. Linear interpolation, smoothing by unweighted moving averages, autocorrelation- and crosscorelation analysis were used in analyzing the data sequences (for the methods, compare J.C. DAVIS, 1986; SCHWARZACHER, 1975).

4.1. Description of the Data Sequences

Raw data sequences of all variables are displayed in Text-Fig. 12 in the interval from –175.10 meters to –237.84 meters of the core. Anomalous behaviour can be seen best in $\delta^{13}C$ with three zones of lowered values (see MAGARITZ & HOLSER, this volume) and in S and P with two zones of increased values. The other variables have a very rugged course indicating major variations among succeeding data points, especially in the two anomalous zones.

Time series procedures require equally spaced data points generated from the irregularly spaced sample

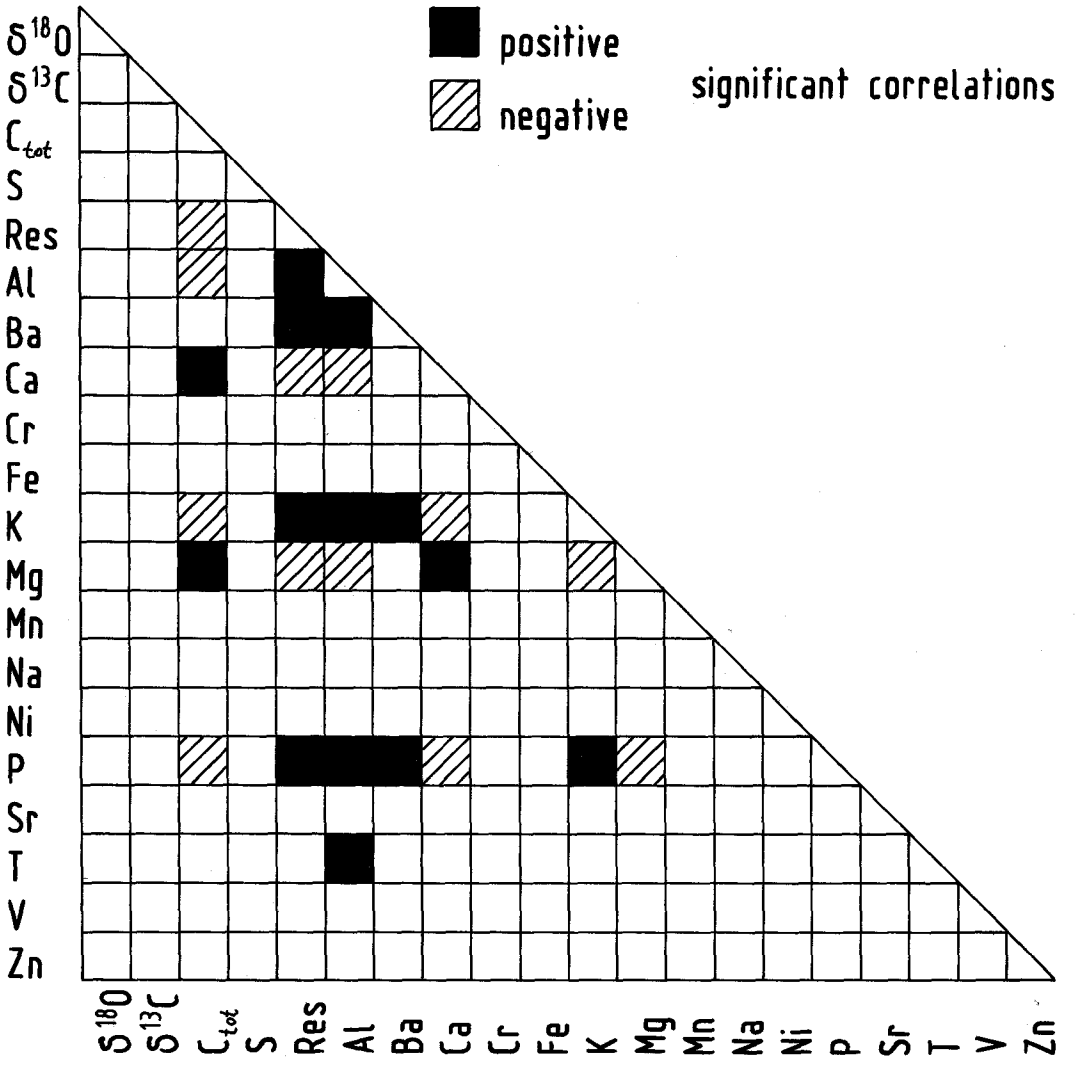

Text-Fig. 8.
Correlation pattern of the general geochemistry data-set including all 332 samples with 20 variables. Correlations significant at the 99 % level are black (positive) or shaded (negative) – see text.

points. For that purpose, 200 data points were linearly interpolated among the 160 sample points. The distance between two interpolated points amounts to 0.315 meters. This point density is sufficient to catch most small-scaled variations.

The interpolated data sequences were smoothed by an unweighted 9-term moving average process in order to emphasize the more obvious and elementary time trends. Text-Fig. 13 shows the smoothed data sequences. Low-value anomalies are shown by $\delta^{13}C$, $\delta^{18}O$ and C_{tot}; the other variables have high-value anomalies – except V which has two large high-value zones separated by a low-value zone. The first anomaly is marked by peaks of the variables in the interval

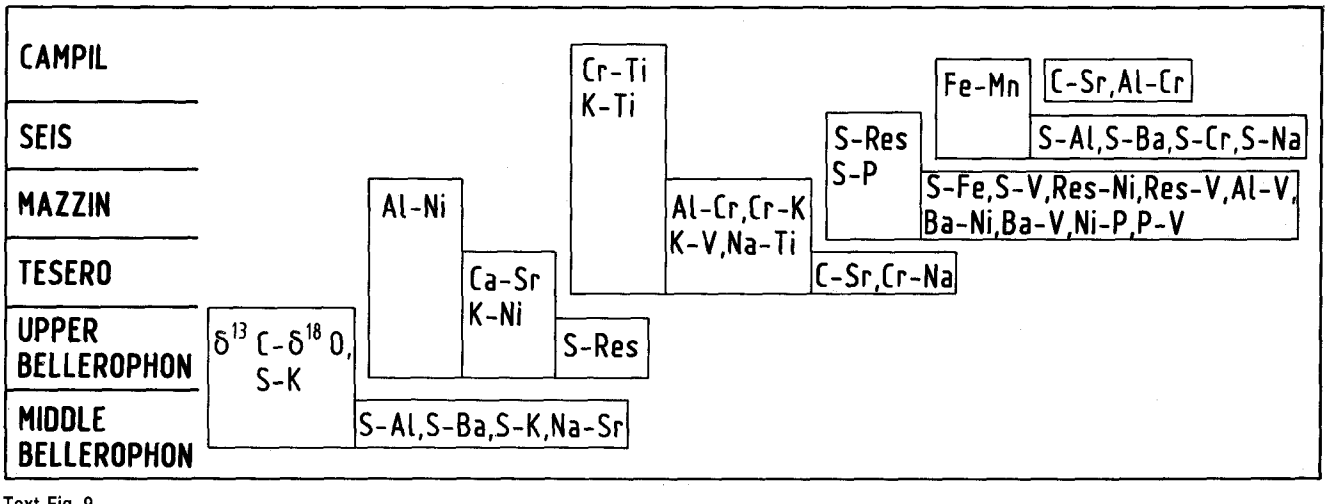

Text-Fig. 9.
Stratigraphic correlation pattern of stratigraphically specific, significant positive correlations (cf. Table 3) which are not contained in the general correlation pattern of Text-Fig. 8.

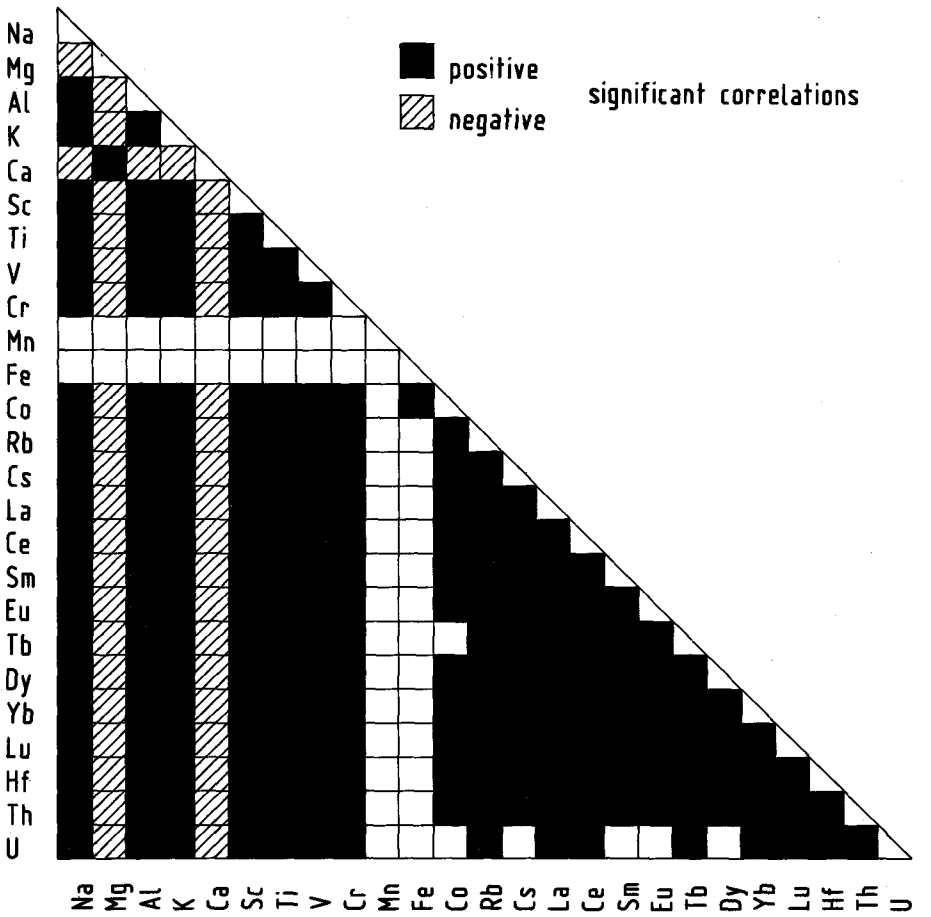

Text-Fig. 10.
Correlation pattern of the INAA data-set including all 72 samples with 25 variables.

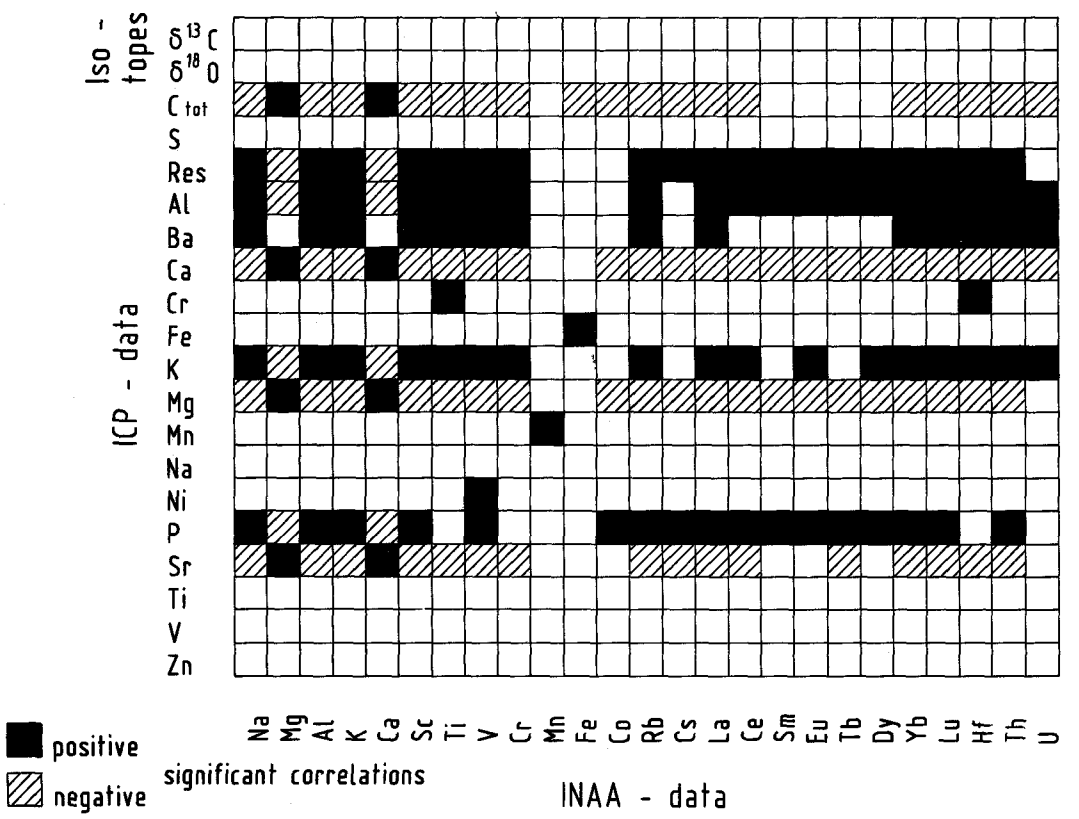

Text-Fig. 11.
Correlation pattern of the isotopes, ICP and INAA data, based on the 72 samples chosen for INAA.

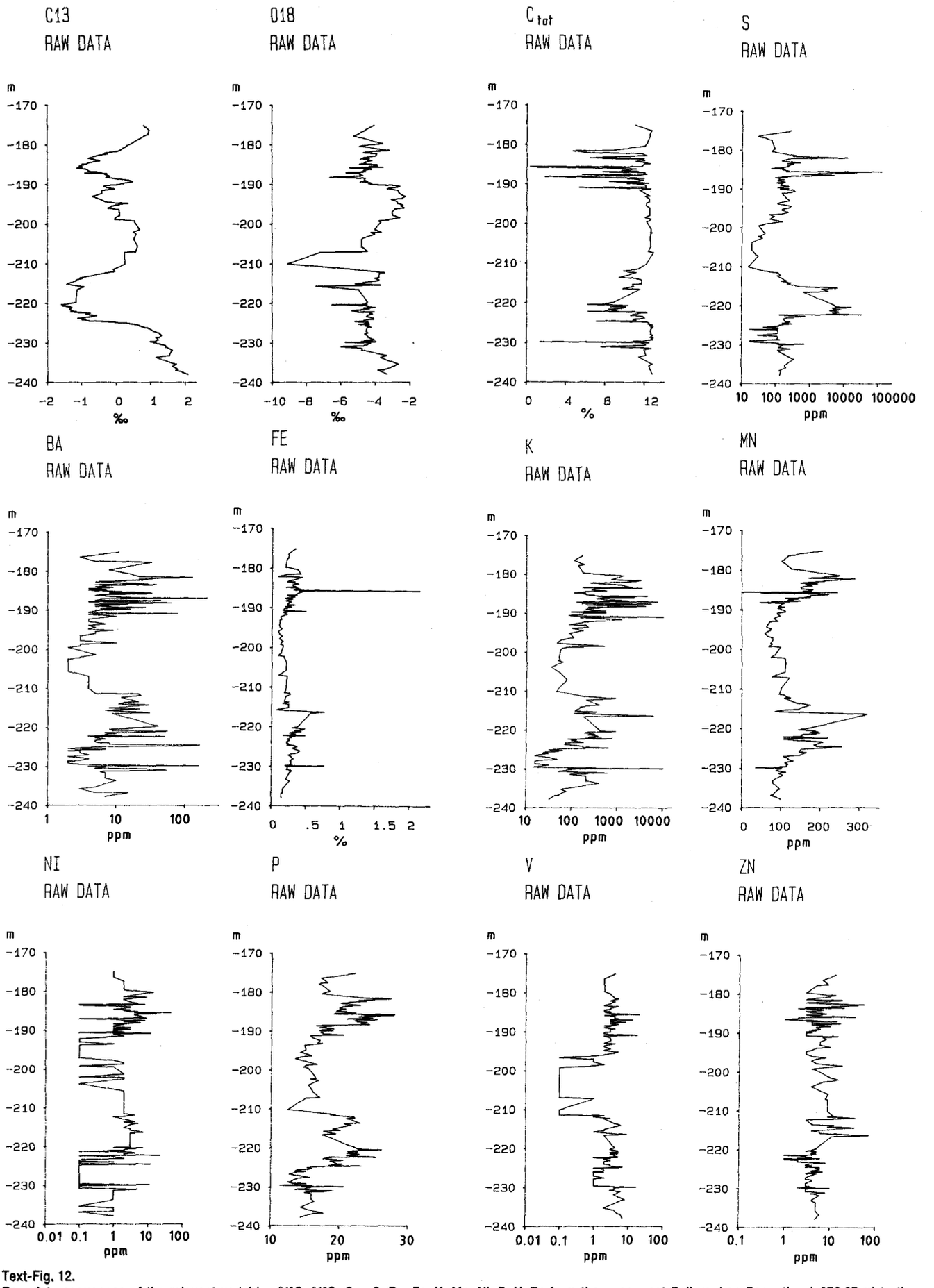

Text-Fig. 12.
Raw data sequences of the relevant variables $\delta^{13}C$, $\delta^{18}O$, C_{tot}, S, Ba, Fe, K, Mn, Ni, P, V, Zn from the uppermost Bellerophon Formation (-278.87 m) to the top of the Mazzin Formation (-175.10 m).

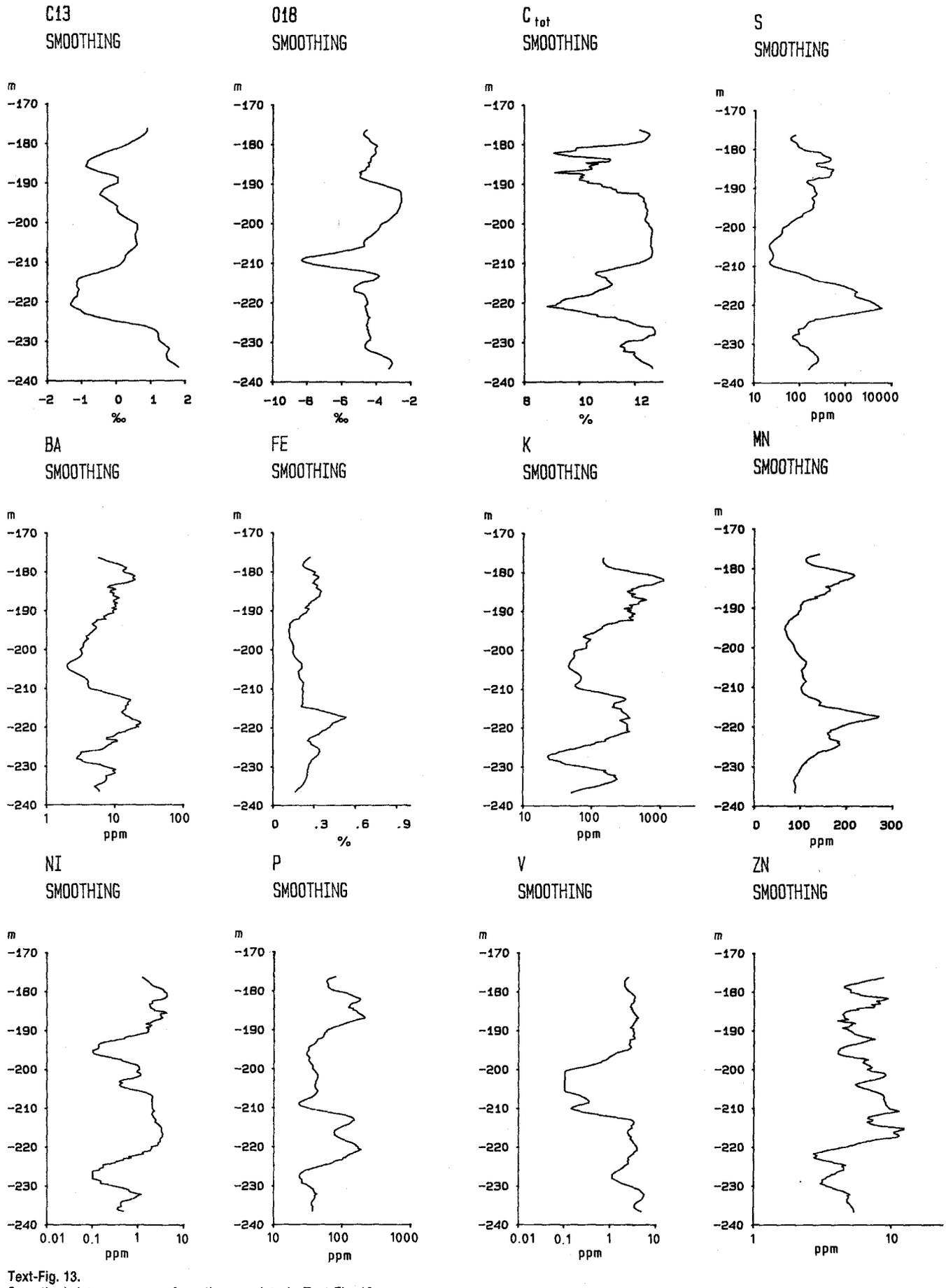

Text-Fig. 13.
Smoothed data sequences from the raw data in Text-Fig. 12.
Smoothing was performed by a 9-term unweighted moving average process.

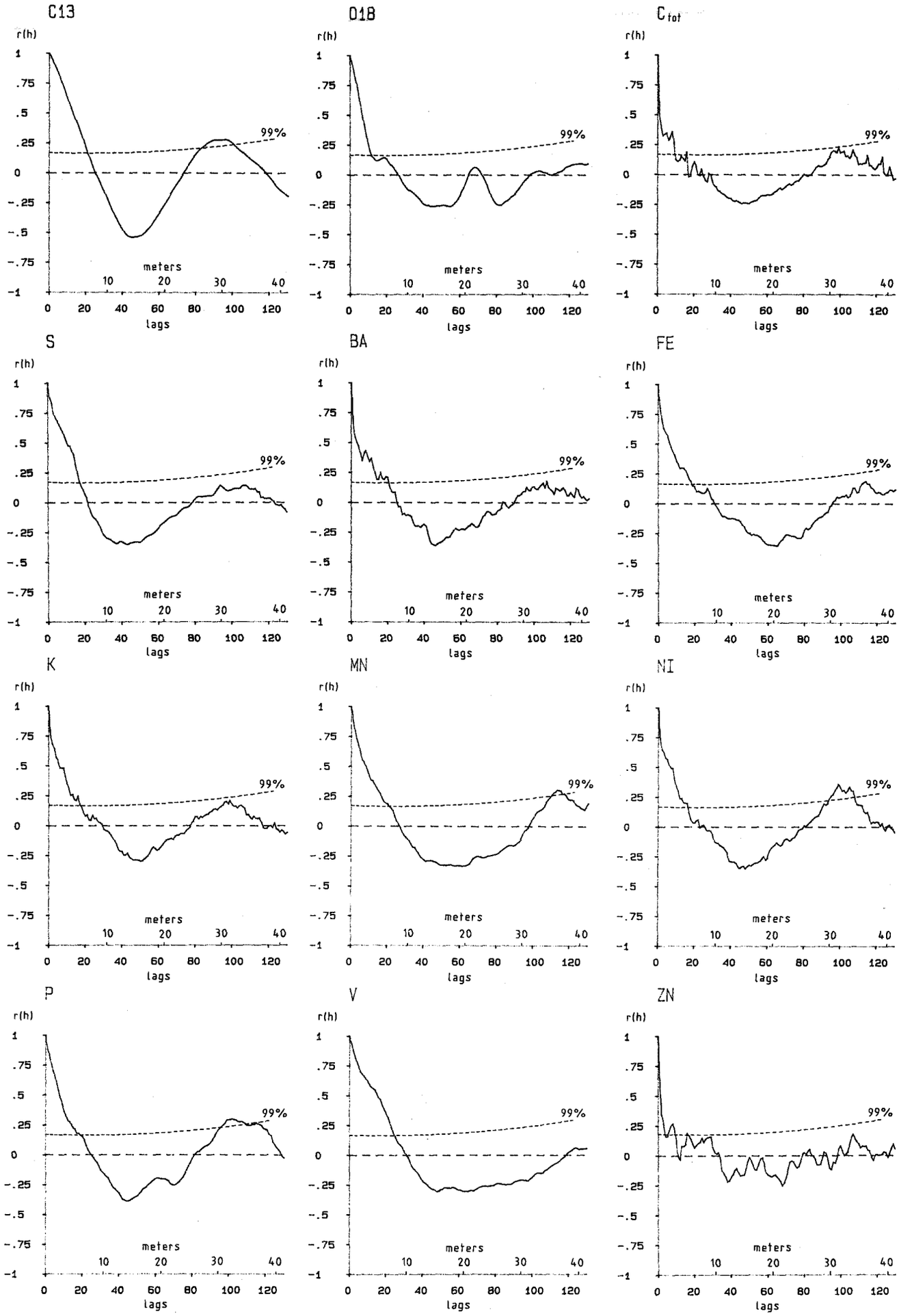

Text-Fig. 14.
Correlograms of $\delta^{13}C$, $\delta^{18}O$, C_{tot}, S, Ba, Fe, K, Mn, Ni, P, V, Zn over a distance of 100 lags or 31.53 m.
r(h) is the correlation coefficient for a given lag.

from −224 to −212 meters. It is best developed on $\delta^{13}C$, $\delta^{18}O$, C_{tot}, S, Ba, K, Mn and P. The anomalous zone is wider for Ni. For $\delta^{18}O$, the first and only significant peak occurs at −209 meters. P has two peaks. Zn shows an oscillating behaviour in the whole section with five peaks between −218 and −181 meters. The second anomaly covers the interval from −188 to −181 meters. The strongest peaks are found in $\delta^{13}C$, C_{tot}, Ba, K, Mn, Ni and P; C_{tot}, S, Ni and P have two peaks.

The first anomaly covers the basal part of the Mazzin Member; in the underlying Tesero Horizon only very few isolated outlier values can be found with C_{tot}, Ba, Fe, K, Ni, P, V. The second anomaly is in the upper part of the Mazzin Member.

4.2. Autocorrelation and Crosscorrelation

Autocorrelation examines the spatial or time influence of a data point on succeeding points. Similarities of data points in dependance of their distance can be determined. Therefore, the autocorrelation structure of the geochemical variables serves to estimate the zone of influence of individual data-points and to detect major oscillations in a data sequence (see K. STATTEGGER, 1988). The empirical autocorrelation function can be displayed graphically in the correlogram with the values of the succeeding correlation coefficients, r(h), for increasing lag in comparing the data sequence to itself.

Using the interpolated data sequences, the correlograms were calculated as exhibited in Text-Fig. 14. Large oscillations indicating the two main anomalous zones can be observed with 99 % significance on $\delta^{13}C$, Mn, Ni, and P. The "upper anomaly" of the smoothed data includes both the second and the third anomalies as described in the chapter on $\delta^{13}C$ and $\delta^{18}O$ isotopes (MAGARITZ & HOLSER, 1989). The lagging distance to reach the second peak in the correlograms varies from 94 to 113 lags, that is, 29.6 to 35.6 meters, which corresponds to the distances between the main anomalies. The zone of influence, that means the shift where the autocorrelation decreases to zero, is for the majority of the variables 22 to 29 lags or 6.1 to 9.1 meters. These distances correspond to the extent of the anomalous zones. Zn has a short zone of influence, 11 lags or 3.4 meters, indicating its individual smaller oscillations. V has a larger zone of influence, 32 lags or 10.1 meters, which is characteristic of the more stable behaviour of this variable.

Although noticeable similarities of the two anomalies can be observed, striking differences remain concerning the "shapes" and the intensities. Therefore, a hypothesized tectonic repetition of the stratigraphic section can be rejected (compare K. STATTEGGER, 1983).

Crosscorrelation analysis was performed using two variables instead of the one used in autocorrelation analysis. $\delta^{13}C$ and $\delta^{18}O$ show a clear shift, see Text-Fig. 15, with a broad peak reaching the maximum at 25 lags, that is 7.9 meters. This corresponds to the distance between the peaks of the two variables in the first anomaly caused by the later occurrence of the $\delta^{18}O$ anomaly. No other shifts could be detected in comparing all variables. We find high positive correlations for $\delta^{13}C - C_{tot}$ and S – Ba – Fe – K – Mn – V,

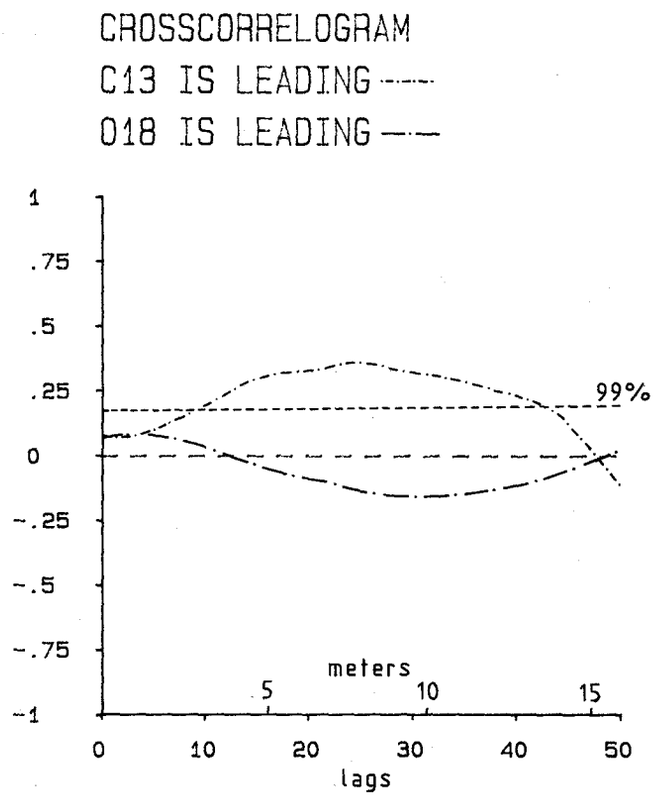

Text-Fig. 15.
Crosscorrelation of $\delta^{13}C$ versus $\delta^{18}O$.

without lagging, indicating a similar course of these variables with respect to the anomalies.

Tests of cyclicity using methods of spectral analysis, especially power spectra (W. SCHWARZACHER, 1984) and Walsh spectra (WEEDON, 1987) did not yield positive results. This indicates that the oscillations are not regularly distributed along the geochemical data sequences and that the main anomalies superimpose all minor oscillations.

4.3. Summary Remarks

Raw data sequences of the relevant variables show in part a rugged course caused by many small-scale oscillations. Smoothing by unweighted moving averages makes the main time trends easier to recognize and gives special evidence of anomalous zones containing lowered or increased values. Two main anomalous zones of some extent can be observed. The first anomaly is located at the basal part of the Mazzin Member, the second anomaly near the top of the Mazzin Member.

The most striking feature of the correlograms is a second positive peak, corresponding to a correlation of the lower anomaly with the upper anomaly. This second maximum is significant for $\delta^{13}C$, Mn, and especially for Ni and P, as indicated by the confidence lines in the correlograms (Text-Fig. 14). Moreover, the lag to the second maximum is very similar for all of these variables, 29 to 31 meters, except Mn whose peak has a longer lag. The peaks in Ni and P (Text-Fig. 13) correspond roughly to the minima in $\delta^{13}C$. The autocorrelations indicates that the structure of the upper anomaly of these elements has much in common with that of

the lower anomaly. This result in turn suggests that the upper and the lower anomalies were generated by similar geochemical processes, especially for Ni and P. Nevertheless, there are sufficient differences in detail of variations of elements through both anomalies to reject an hypothesis that the lower and upper anomalies represent a tectonic repetition of the stratigraphic section.

A shift is noticeable between $\delta^{13}C$ and $\delta^{18}O$, proved by cross correlation analysis, due to the later occurrence of the first anomaly on $\delta^{18}O$.

References

AITCHISON, J.: The Statistical Analysis of Compositional Data. – 416 pp., London (Chapman and Hall) 1986.

DAVIS, J.C.: Statistics and Data Analysis in Geology, 2nd ed. – 646 pp., New York (Wiley) 1986.

HITCHON, B. & FILBY, R.H.: Use of Trace Elements for Classification of Crude Oils into Families – Example from Alberta, Canada. – Am. Ass. Petr. Geol. Bull., **68**, 838–849, Tulsa 1984.

JENNRICH, R.I.: Stepwise Discriminant Analysis. – In: ENSLEIN, K., RALSTON, A. & WILF, H.S. (Eds.): Statistical Methods for Digital Computers, 454 pp., New York (Wiley) 1977.

KREYSZIG, E.: Statistische Methoden und ihre Anwendung. – 451 pp., Göttingen (Vandenhoek & Ruprecht) 1979.

KRZANOWSKI, W.J.: The Performance of Fisher's Linear Discriminant Function Under Non-Optimal Conditions. – Technometrics, **19**, 192– 208, 1977.

REYMENT, R.A., BLACKITH, K.E. & CAMPBELL, W.A.: Multivariate Morphometrics. – 233 pp., London (Academic Press) 1984.

SCHWARZACHER, W.: Sedimentation Models and Quantitative Stratigraphy. – Dev. Sedimentology, **19**, 382 pp., Amsterdam (Elsevier) 1975.

SCHWARZACHER, W.: Models for Induced Cyclic Sedimentation. – Proc. 27th Geol. Congr., **20**, 85–104, Moscow 1984.

STATTEGGER, K.: Application of Time Series Analysis to the Tectonic Analysis of Disturbed Rock Sequences Recorded from Drill Hole Logs with Examples from the Paleozoic of Graz (Austria). – Math. Geology, **15**, 673–685, New York 1983.

STATTEGGER, K.: Stream sands – Modeling of Deposition Using Multivariate Statistics and ARMA-Processes. – Sci. de la Terre, Ser. Inf., **27**, 439–453, Nancy 1988.

VELLEMAN, P.F. & HOAGLIN, D.C.: Applications, Basics and Computing of Exploratory Data Analysis. – 354 pp., Boston (Duxbury press) 1981.

WEEDON, G.P.: Hemipelagic Shelf Sedimentation and Climatic Cycles: the Basal Jurassic (Blue Lias) of South Britain. – Earth Planet. Sci. Lett., **76**, 321–335, Amsterdam 1986.